

Effects of the grain size distribution on the temperature-dependent magnetic susceptibility of magnetite nanoparticles

ZHAO XiangYu^{1,2} & LIU QingSong^{1*}

¹ Paleomagnetism and Geochronology Laboratory (SKL-LE), Institute of Geology and Geophysics, Chinese Academy of Sciences, Beijing 100029, China;

² Graduate University of Chinese Academy of Sciences, Beijing 100049, China

Received November 24, 2009; accepted March 16, 2010; published online June 1, 2010

Magnetite is an important magnetic remanence carrier in natural samples and therefore is of great interest in paleo-, rock-, and environmental magnetism. The magnetic properties of magnetite depend on many factors, e.g., concentration and grain size distribution (GSD). In this study, we theoretically investigated the temperature-dependent susceptibility (TDS) of magnetite nanoparticles with a lognormal GSD. Results show that the TDS is affected highly by the GSD mainly in three aspects. Firstly, the unblocking process becomes smoother with the increase of distribution width, characterizing as a wider Hopkinson peak on the TDS curve. Secondly, the blocking temperature increases with the increase of the median diameter or/and the distribution width. Thirdly, the maximum susceptibility decreases with the increase of distribution width, and has a logarithmic function relation with the standard deviation of the distribution. As a case study, this model was further applied to the thermal products of the Chinese loess/paleosol samples to determine the granulometry of newly-formed magnetite upon heating based on TDS curves. The results demonstrate the fidelity and feasibility of this method to determine the GSD of nano-sized magnetic particles.

Néel theory, temperature dependence of susceptibility, grain size distribution

Citation: Zhao X Y, Liu Q S. Effects of the grain size distribution on the temperature-dependent magnetic susceptibility of magnetite nanoparticles. *Sci China Earth Sci*, 2010, 53: 1071–1078, doi: 10.1007/s11430-010-4015-y

Iron oxides (magnetite, maghemite, hematite, and goethite) are common in natural environments, such as soils, rocks and sediments. The formation and preservation of these magnetic minerals are affected highly by the ambient environment, and hence the magnetic signals are excellent environmental proxies [1, 2]. More specifically, composition, concentration, and the grain size distribution of the magnetic minerals have been widely used in environmental studies [3, 4].

Magnetic susceptibility (χ , mass-specific, or κ , volume-specific) measures the response of a material to an

external magnetic field [5], and is comprehensively utilized in environmental studies. In paleoceanographic study, magnetic susceptibility of marine sediments helps to understand the paleoclimate changes [4]. For example, distinct peaks of magnetic susceptibility of marine sediments in North Atlantic during the last glacial period were associated with Heinrich layers, which reflect ice sheet dynamics [6]. Magnetic susceptibility of the Chinese loess-paleosol sequence correlates well to the oxygen isotope record of deep-sea cores [7], thus providing good records for the research of terrestrial paleoclimate. Meanwhile, the temperature dependence of magnetic susceptibility ($\chi-T$ or $\kappa-T$) has been used to detect magnetic compositions, domain states, average grain size, and phase transition during the thermal

*Corresponding author (email: liux0272@yahoo.com)

treatment [8, 9]. For example, Deng et al. [9] suggested that magnetite and maghemite are dominant magnetic carriers in the Chinese loess and paleosols, and that the descending of heating χ - T curve around 300–450°C is caused by transition of maghemite to hematite, and magnetite is responsible for the ascending around 510°C. They concluded that the two phenomena manifest the degree of pedogenesis and thus are climatically indicative. On the basis of the χ - T curves, it is suggested that there is an analogy between heating process and pedogenesis [8, 9]. Recently, Liu et al. [10] constructed the continuous grain size distribution of the newly-formed magnetite during heating by using the temperature-dependent of magnetic susceptibility measured at dual frequencies (1 and 10 Hz) [11].

Magnetic susceptibility of a specific kind of iron oxides is usually a function of several factors, including concentration, composition, magnetic interaction, grain shape, grain size (domain state), distribution, temperature, and the working frequency [1–5, 12]. In order to understand these effects, extensive rock-magnetic studies have been carried out using both synthetic magnetic samples and theoretical simulation. For example, Maher [1] investigated magnetic properties of synthetic nano-sized magnetites, and concluded that magnetites with a mean grain size of ~20 nm show the maximum frequency dependence of susceptibility ($\chi_{fd}\%$) and that those of ~50 nm have maximum intensity of anhysteresis remanent magnetization (ARM, or normalized form, χ_{ARM}). Thus, the combination of $\chi_{ARM}/SIRM$ (saturation remanence) and $\chi_{fd}\%$ can distinguish the superparamagnetic (SP) particles and coarse multi-domain (MD) grains. Based on Maher's conclusion, Zhou et al. [13] suggested that the magnetic enhancement in the Chinese paleosols results from the fine magnetic particles produced by pedogenesis.

However, synthetic samples usually have a rather wide grain size distribution and strong magnetic interactions, and thus yield discrepancies when interpreting the corresponding magnetic signals. Instead, theoretical simulation is an alternative approach. For example, magnetic susceptibility of SP particles is frequency-dependent [10, 14–17]. The magnetic susceptibility decreases with the increasing measure frequency [16, 17]. The difference between χ_{lf} , measured at low frequency, and χ_{hf} , measured at high frequency, is χ_{fd} . In addition, for a specific mean grain size, a narrower distribution gives rise to a higher $\chi_{fd}\%$ value, whereas $\chi_{fd}\%$ itself is not sufficient to inversely deducing the magnetic granulometry [14, 15], as particles with diverse distributions could have same $\chi_{fd}\%$ [15]. Therefore, other parameters are needed for the magnetic granulometry [14], e.g., the temperature dependence of χ_{fd} is helpful to acquire the distribution of SP+SD (single domain) samples [10, 17].

Further studies suggested that grain size distributions have effects on the κ - T curves [1, 14]. As it is reported that the lognormal grain size distribution is common in natural

samples [18, 19], the present paper focuses on variations of the κ - T curves aroused by SP+SD magnetites with diverse lognormal volume distributions on the basis of previous studies, and propose a magnetic granulometry approach.

1 Theory

With the increase of the grain size, the domain states of ferrimagnetic grains are divided up into SD, pseudo single domain (PSD), and MD [2]. For SD particles, they are further classified into three states: superparamagnetic (SP), viscous superparamagnetic (VSP), and stable single domain (SSD). SP particles are affected by thermal activation so much that their easy axes are randomly distributed in a zero field and that are very sensitive to external magnetic fields, while SSD assemblages possess the high enough energy barriers to overcome thermal agitations and thus have a lower susceptibility [17].

The relaxation time (τ) measures the stability of the moment of a SSD particle [14, 17]:

$$\tau = \tau_0 \exp\left(\frac{KV}{kT}\right), \quad (1)$$

where τ_0 is the pre-exponential time constant, often used as $\tau_0=10^{-9}$ s for magnetite [14, 17], K is the anisotropy constant, V is the volume of the particle, thus KV represents the energy barrier, and k is the Boltzmann constant, kT is the thermal energy. For uniaxial magnetite, the shape anisotropy contributes dominantly to the energy barrier [14] so that:

$$K = \mu_0 M_s H_k / 2, \quad (2)$$

where μ_0 is the vacuum permeability, and $\mu_0=4\pi\times 10^{-7}$ H/m in the SI system, M_s is the saturation magnetization, and H_k is the microscopic coercivity.

Combining eqs. (1) and (2), we obtain

$$V = \frac{2kT}{\mu_0 M_s H_k} \ln\left(\frac{\tau}{\tau_0}\right). \quad (3)$$

Note that if τ is less than the measuring time, the moments are disordered, i.e., in the SP state. Defining $\omega\tau_b=1$ as the critical state between SP and SD states, and substituting τ_b into eq. (3), we obtain the blocking volume V_b below which the moments are disordered when measured. Correspondingly, it is assumed in the present calculation that within an assemblage of same H_k , particles with volume less than V_b is SP, otherwise SD.

If magnetic interactions are negligible, SSD particles have susceptibility [14]:

$$\kappa_{SD} = \frac{2M_s}{3H_k}. \quad (4)$$

SP particles have AC susceptibility [14]:

$$\kappa_{SP} = \frac{1}{(1 + \omega^2 \tau^2)} \frac{\mu_0 V M_s^2}{3kT}. \quad (5)$$

Besides, M_s and H_k vary with temperature as follows [17]:

$$\frac{M_s(T)}{M_{s0}} = \left(\frac{T_c - T}{T_c - T_0} \right)^m, \quad (6)$$

$$\frac{H_k(T)}{H_{k0}} = \left(\frac{T_c - T}{T_c - T_0} \right)^n, \quad (7)$$

where T_0 is room temperature (~300 K), and for magnetite with dominant shape anisotropy, $n=m \approx 0.43$ [17], M_{s0} is the saturation magnetization at room temperature, and equals to 478.4 kA/m for magnetite, $H_k(T)$ can be evaluated by the measurable macroscopic coercivity $H_c(T)$ [17]:

$$H_k(T) = 2.09H_c(T). \quad (8)$$

For an assemblage with grain size distribution of $N(V)$, the susceptibility is the average of those of all particles [15, 16]:

$$\begin{aligned} \kappa_{avg} &= \frac{\sum \kappa(V)N(V)V}{\sum N(V)V} \\ &= \frac{\sum_{V_{min}}^{V_b} \kappa_{SP}(V)N(V)V + \sum_{V_b}^{V_{max}} \kappa_{SD}N(V)V}{\sum N(V)V}, \end{aligned} \quad (9)$$

where $\kappa(V)$ is the susceptibility of particles with volume V , $N(V)$ is the probability density function of a distribution, V_{min} and V_{max} are minimum and maximum volume, respectively.

As the lognormal distributions are very common in natural samples [18, 19], e.g., pedogenesis-generated fine ferromagnetic particles [10], we assumed the assemblages calculated in the paper follow lognormal distributions [15, 18]:

$$N(V) = f(V, V_m, \sigma) = \frac{1}{\sqrt{2\pi}\sigma V} \exp\left(-\frac{(\ln V - \ln V_m)^2}{2\sigma^2}\right), \quad (10)$$

where V_m is the median volume and σ^2 the variance [18].

Then the temperature dependence of susceptibility of non-interacting magnetite can be calculated with eqs. (1) to (10).

2 Results and discussions

The variation of magnetic susceptibility of magnetite with volume at room temperature is illustrated in Figure 1. For particles with volume of V and coercivity of 25 mT, magnetic susceptibility increases with increasing V linearly, and

decrease sharply around ~20 nm. When the grain size distribution is considered, its maximum decreases considerably, and it reaches the maximum more sharply but decreases more smoothly after crossing the SP/SD threshold.

The κ - T curves of magnetite assemblages with the same grain size distribution ($D_m=16$ nm, $\sigma=0.3$) but with different coercivities are shown in Figure 2. For the assemblage with coercivity $B_c=30$ mT, the magnetic susceptibility remains stable below 100 K, above which particles start unblocking, and reach their peak value around 300 K. It decreases all the way above 300 K until its Currie temperature (T_c) where magnetite becomes paramagnetic. As coercivity increases, e.g., $B_c=50$ mT shown in Figure 2, the initial value decreases, particles become unblocked and reach the maximum susceptibility at elevated temperatures, 200 and 400 K respectively. However, the two curves are merged after 500 K.

Figure 2 demonstrates that higher coercivity increases the blocking temperature (T_b) and decreases the susceptibility

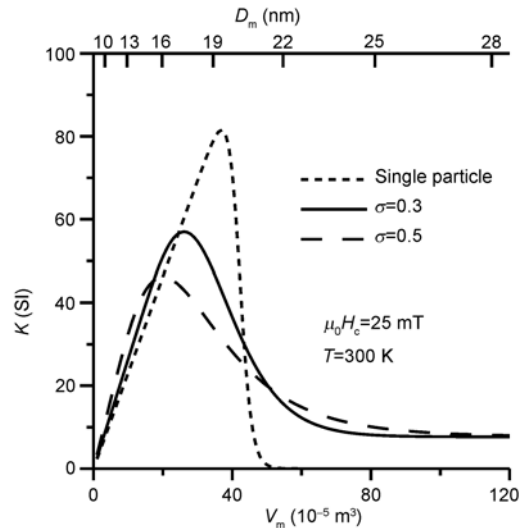


Figure 1 Variations in magnetic susceptibility with respect to the median volume at room temperature (300 K). The coercivity of the magnetite particles is set to 25 mT.

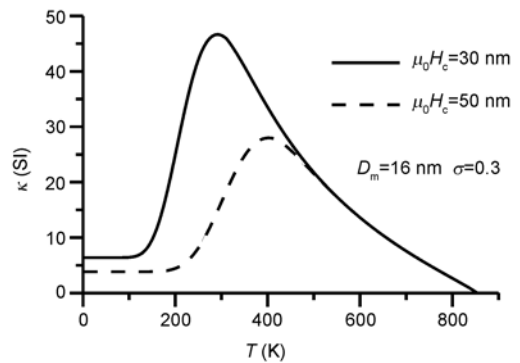


Figure 2 κ - T of magnetite assemblages with different coercivities. These two curves are calculated using the same grain size distribution ($D_m=16$ nm and $\sigma=0.3$).

of particles in the blocking state. Referring to eqs. (1) and (2), we know that for a given τ , SD particles with higher coercivities possess higher energy barriers, to overcome which more thermal energy, hence higher temperature, is required. After unblocking, the particles are in the SP state, and the effect of coercivity on susceptibility disappears, as seen in eq. (5), so the susceptibilities are the same.

κ - T curves of magnetite assemblages with different median grain sizes but the same variance are displayed in Figure 3. Since SP particles are dominant in the assemblage with $D_m=12$ nm, its susceptibility increases at 100 K and has a lower T_b around 120 K, and as D_m increases, SD particles become predominant and T_b increases, e.g., for the assemblage with $D_m=28$ nm, particles start unblocking above 500 K and the T_b is ~ 600 K. However, all assemblages have the same peak value at every T_b , i.e., same $\kappa(T_b)$. As dash lines in Figure 3 demonstrated, T_b shifts rightward and $\kappa(T_b)$ decreases with increasing σ , and that the unblocking process becomes smoother, i.e., with a wider peak. Besides, despite different σ , the initial values before unblocking are same, indicating that the value is dependent not on the grain size distribution but on the coercivity.

Five κ - T curves of magnetite assemblages with the same median diameter but different variances are depicted in Figure 4(a), which shows that as σ increases, unblocking

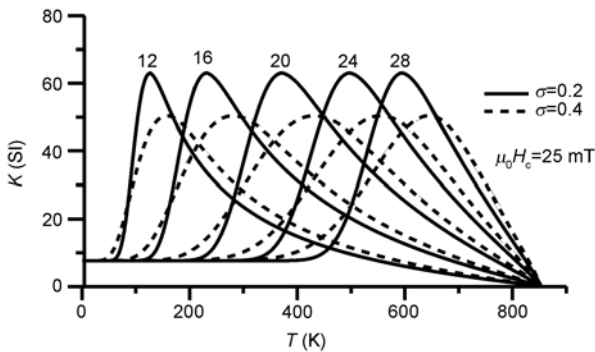
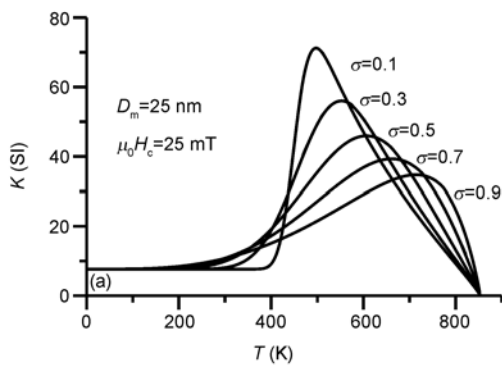


Figure 3 κ - T of magnetite particles with different σ . The numbers above curves indicate the median diameters (unit: nm). The coercivity of all particles is set to 25 mT.



occurs at a lower temperature more smoothly with a T_b closer to T_c , resulting a wider Hopkinson peak [20, 21]. Corresponding grain size distributions are displayed in Figure 4(b).

As qualitatively demonstrated above, it is clear that coercivity and grain size distribution have significant effects on the temperature dependence of susceptibility. Trying to quantify the effects, we reorganized simulation data in Figure 5(a), where $\kappa(T_b)$, i.e., κ_{max} , of five magnetite assemblages of different B_c are plotting versus σ , showing that the increase of both B_c and σ can give rise to decreasing κ_{max} . By fitting to these data, we found that κ_{max} and σ follow the logarithmic relation:

$$\kappa_{max} = B \ln \sigma + A.$$

Though A and B are different for diverse B_c , they seem to be a function of B_c according to the fitted data displayed in Figure 5(b). Then we proposed the following relation for lognormally distributed SP+SD magnetite assemblages with identical coercivity:

$$\kappa_{max} = B \ln \sigma + A, \tag{11}$$

$$A = 837.356(\mu_0 H_c)^{-1}, \tag{12}$$

$$B = -434.448(\mu_0 H_c)^{-1}. \tag{13}$$

As D_m has an effect on the shifting of T_b for a given σ , D_m data are plotted versus T_b for diverse σ . In Figure 5(c) and (d) are data of magnetite with $B_c=30$ mT and 50 mT, respectively. There is only qualitative relation already explained above, i.e., T_b increases with the increase of D_m for a given σ , which also has significant effects on T_b . Nevertheless, it reminds us that estimating D_m simply by T_b may give rise to significant errors. For example, in Figure 5(d), the difference between T_b ($\sigma=1.0$) and T_b ($\sigma=0.1$) is more than 200 K given $D_m=20$ nm and that between D_m ($\sigma=0.1$) and D_m ($\sigma=1.0$) exceeds 10 nm given $T_b=700$ K. However, wide grain size distributions are quite common for natural samples [14, 22]; in this case, estimating by T_b is acceptable

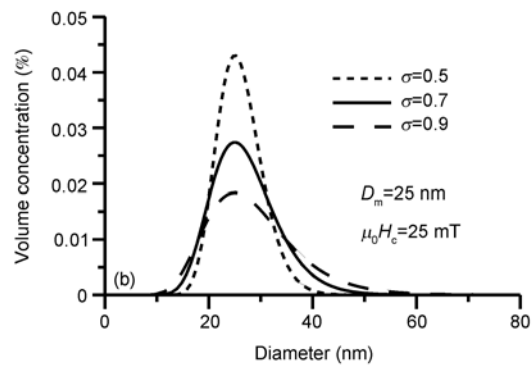


Figure 4 κ - T of magnetite particles with different σ . (a) κ - T curves. $D_m=25$ nm, σ is marked next to the corresponding curve. The coercivity $B_c=25$ mT. (b) Grain size distributions of corresponding assemblages with $\sigma=0.5, 0.7, 0.9$ respectively in (a).

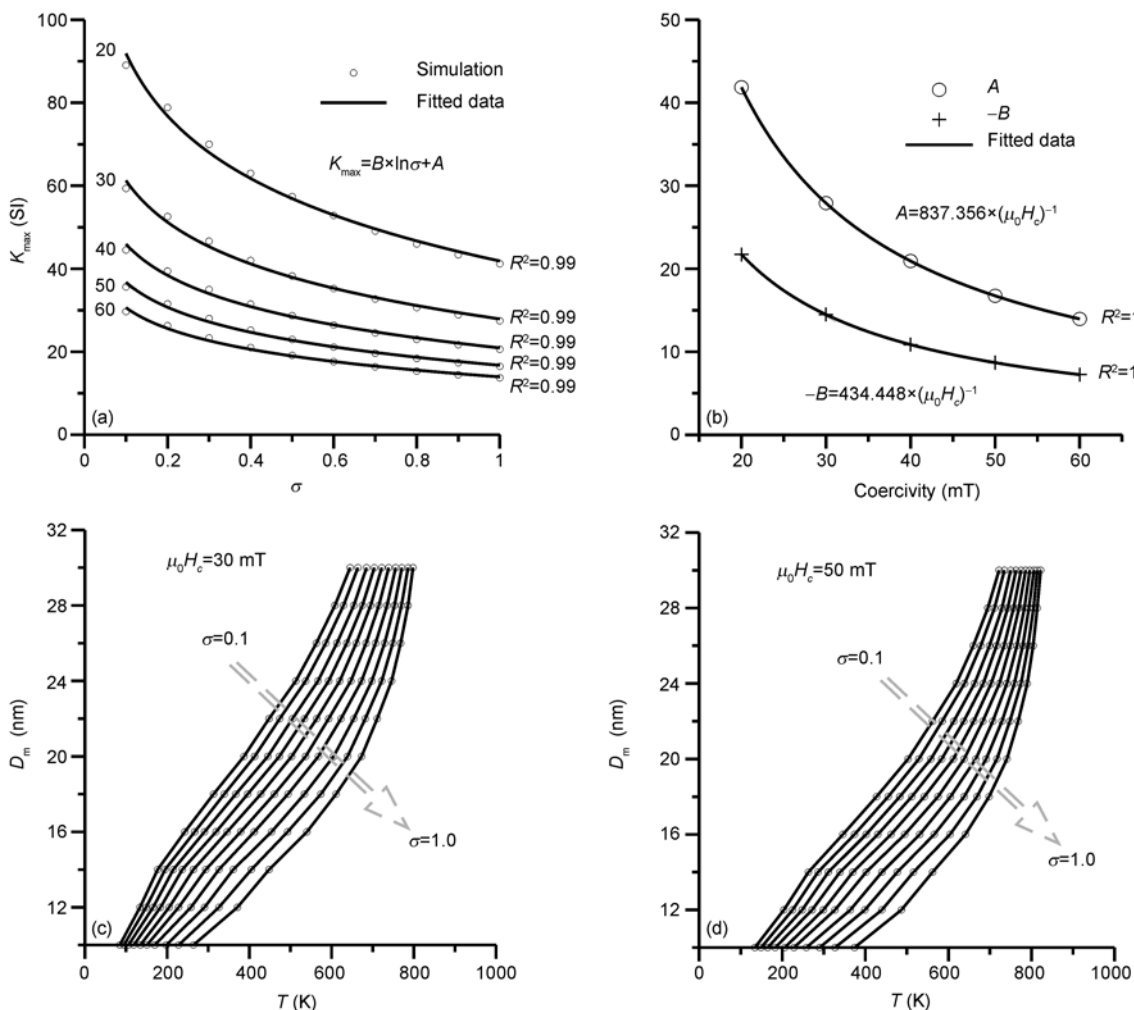


Figure 5 Effects of coercivity and grain size distribution on κ - T curves. (a) Numbers on the left of curves refer to B_c . κ_{max} and σ follow logarithmic relation, R^2 is the determinant coefficient; (b) coefficients A and B versus $\mu_0 H_c$. Fitted results imply that A and B are inversely proportional to $\mu_0 H_c$; (c) and (d) D_m of magnetite with diverse σ versus T_b , σ varies from 0.1 to 10.

practically as illustrated in Figure 5(d) for example, where the difference of about 3 nm between D_m ($\sigma=0.7$) and D_m ($\sigma=0.9$) was found at $T_b=700$ K.

In fact, low-temperature and high-temperature κ - T are separately measured in laboratory, and they take on distinguishing characteristics for SP and SD particles as their T_b are different, thus it is necessary to investigate these two curves separately.

As illustrated by Maher's experiments [1], there is a significant increase in low-temperature κ - T curves of SP particles, suggesting that it is a useful method to detect the presence of SP components. This is observed also in the simulation as shown in Figure 6(a). For very fine-grained particles, T_b may still be restricted in low-temperature range even with a wide distribution, e.g., $D_m=10$ nm, $\sigma=0.9$. For larger SP assemblages, e.g., with $D_m=18$ nm and $\sigma=0.3$, $\sigma=0.9$, magnetic susceptibility increases conspicuously and may not reach peak value until 300 K. In contrast, magnetic susceptibility of an SD assemblage, e.g., with $D_m=25$ nm

and $\sigma=0.3$, does not change much, unless sufficient SP components are intermingled (e.g. $D_m=25$ nm and $\sigma=0.9$, grain size distribution is illustrated in Figure 4(b)).

As T_b of SD particles is more than 300 K (Figure 3), SD components are easily recognized in high-temperature κ - T curves. For example, 25 nm (0.3) and 35 nm (0.3) in Figure 6(b) are two representative curves with Hopkinson peaks. Coarser SD particles have Hopkinson peaks closer to T_c as explained by eq. (1), whereas susceptibility of SP particles decreases as soon as crossing T_b below room temperature. Thus, it follows a descending trend different from that of neither SD nor MD particles at high temperature as shown in Figure 6(b).

3 Applications

3.1 A case study for the thermal products of the Chinese loess-paleosols

The Chinese loess and paleosols contain pedogenically-

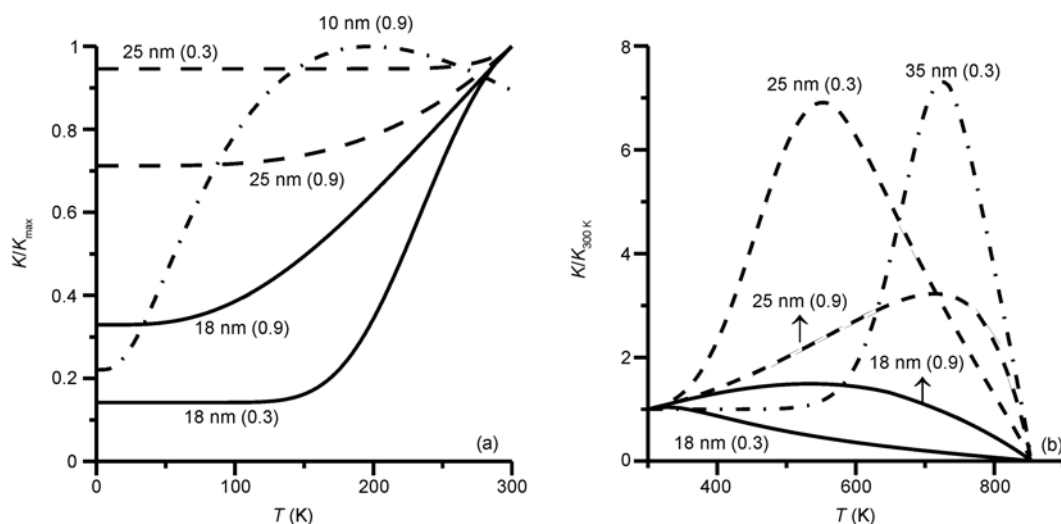


Figure 6 Low- and high-temperature κ - T curves. (a) Low-temperature κ - T curves normalized to the max volume susceptibility (κ_{\max}) in the range from 0 to 300 K; (b) High-temperature κ - T curves normalized to κ_{300K} . Marked numbers refer to D_m (σ).

generated SP and SD particles, which are analogous to those produced during heating process in an argon environment [8, 13]. Thus, it is important to determine the grain size distribution of the thermal products of the Chinese loess-paleosol samples. The κ - T curves of samples from Yuanbao, Linxia ($35^{\circ}38'N$, $103^{\circ}10'E$) are plotted in Figure 7(a), which are representative of loess/paleosol samples. For the heating curve (Figure 7(a)), the decrease of magnetic susceptibility above $300^{\circ}C$ is believed to be caused by the conversion of strongly ferrimagnetic maghemite to weakly antiferromagnetic hematite and the peak value after $500^{\circ}C$ is mainly the consequence of neoformation of ferrimagnetic minerals dominated by magnetite as the T_c is $580^{\circ}C$ [9]. The other two solid lines represent cooling κ - T curves of the identical primitive samples heated to 500 and $600^{\circ}C$ respectively. The dash line is made by subtracting the $500^{\circ}C$ curve from the $600^{\circ}C$ one, representing contributions of magnetite fraction generated between 500 and $600^{\circ}C$. Simulation result is compared to this curve as displayed in Figure 7(b). It is shown that simulation result fits well to the measured data above $300^{\circ}C$. The dash-and-dot line is the difference, and it resembles the pattern shown in Figure 6(b) with $D_m=18$ nm and $\sigma=0.3$, which possibly indicates the presence of finer components or diverse grain size distributions, e.g., Weibull distribution [23]. However, the difference may also be concerned with the presence of maghemite and of interactions among newborn magnetite. Nevertheless we believed it is an acceptable result and the corresponding lognormal grain size distribution is represented in Figure 7(c), with $D_m=26$ nm and $\sigma=0.78$, which is comparable to ferrimagnetic minerals of pedogenesis origin [8, 17].

3.2 Limitations

Firstly, the compositions of natural samples are usually very

complex, including paramagnetic clays, ferrimagnetic and antiferromagnetic minerals (e.g., hematite and goethite [24]). Thus, κ - T curves will be complicated in the case of the mixture of different magnetic components in competitive amount. Secondly, since magnetic susceptibility of coarse particles (PSD and MD) remain relatively stable with respect to temperature, this may account for, at least partially, the discrepancy between simulation and measured data below $200^{\circ}C$ in Figure 7(b). Thirdly, antiferromagnetic contributions may be significant at lower temperatures. Although antiferromagnetic susceptibility is generally lower than ferrimagnetic susceptibility above the room temperature, it could be enhanced considerably by the effect of uncompensated moments at lower temperatures [25]. The complexities mentioned above have not been taken into account in the present model.

In contrast, as only fine particles are responsible for low-temperature frequency dependence of susceptibility [10] signal, other influences are removed implicitly, which ensures the inversion of grain size distributions of fine maghemite particles of pedogenesis origin. However, as the limitations of the equipments, e.g., the MPMS system, maximum measuring temperature available is 400 K, which in turn limits the detection of larger grain sizes. Therefore, the two approaches are considered complementary.

4 Conclusions

The above calculations and analyses have demonstrated that the grain size distribution has significant effects on the temperature dependence of susceptibility of fine magnetite assemblages. For the lognormal distribution, we found:

- (1) For a given σ , T_b increases with the increase of D_m .
- (2) For a given D_m , with the increase of σ , T_b increases

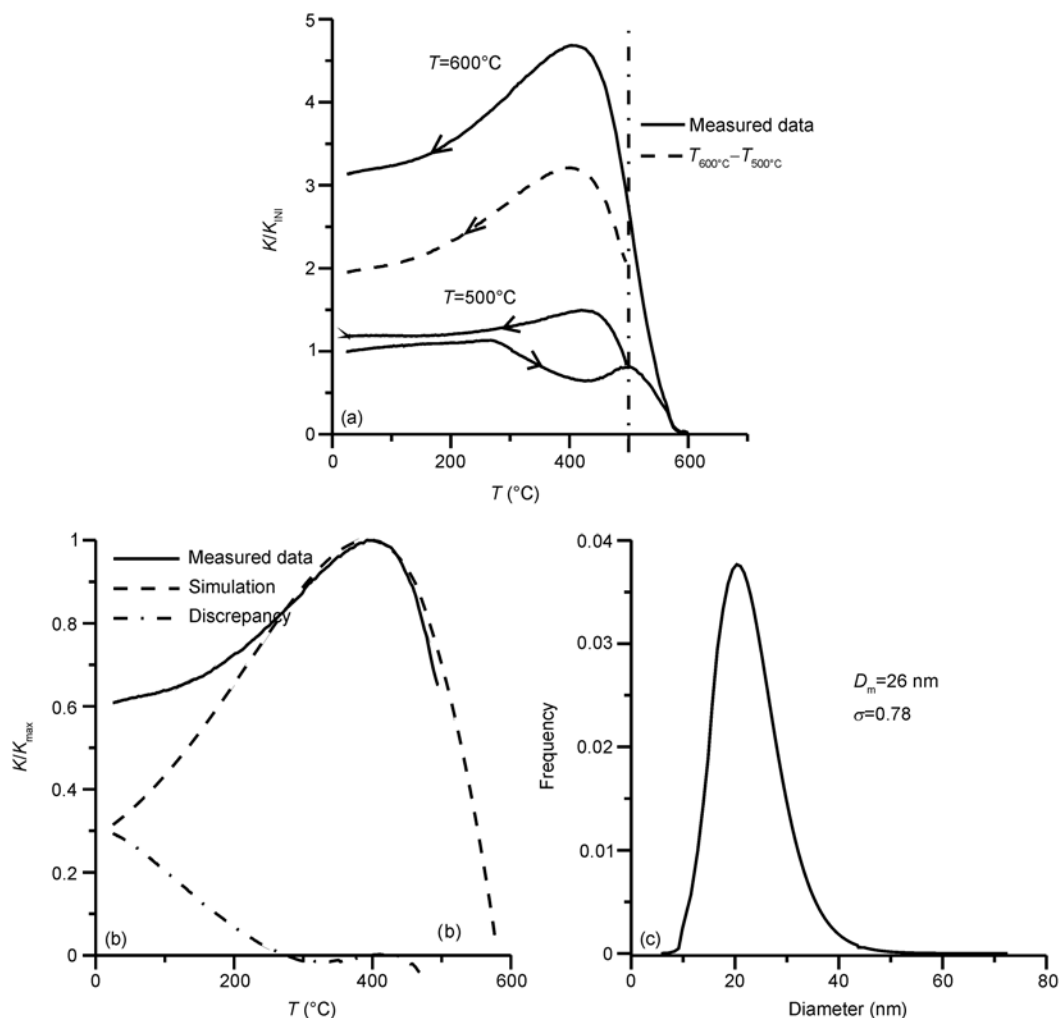


Figure 7 Grain size distribution of the thermal products of Chinese loess-paleosol samples. (a) Partial heating/cooling κ - T curves. Normalized to magnetic susceptibility at room temperature of the primitive sample (κ_{INI}). The dash line is made by subtracting the 500°C curve from the 600°C one. (b) Simulation result vs. measured data. The solid line is identical to the dash line in (a), representing contributions of newborn magnetite generated between 500 and 600°C. The dash line is best-fitted result by the present simulation. The dash-and-dot line is the discrepancy; (c) Grain size distribution corresponding to the best-fitted result.

while κ_{max} decreases, and κ - T curve becomes smoother with a wider Hopkinson peak.

(3) κ_{max} and σ follow the relation of $\kappa_{max}=B\ln\sigma+A$, where B and A are functions of coercivity.

Given the commonality of lognormal distributions in natural samples, this model can be used to fit the measured κ - T curves of samples containing dominant SP+SD magnetite in order to acquire grain size distributions.

We thank two anonymous reviewers for their comments on the previous version of the manuscript, and Drs. Qin Huafeng, Li Zhenyu, and Cao Changqian for valuable discussions. This work was supported by National Natural Science Foundation of China (Grants Nos. 40974036 and 40821091) and the CAS/SAFEA International Partnership Program for Creative Research Teams. Liu Qingsong acknowledges further support from the 100-talent Program of the Chinese Academy of Sciences.

1 Maher B A. Magnetic properties of some synthetic sub-micron mag-

netites. *Geophys J*, 1988, 94: 83–96

- 2 Dearing J A. *Environmental Magnetic Susceptibility: Using the Bartington MS2 System*. Kenilworth: Chi Publishing, 1994
- 3 Evans M E, Heller F. *Environmental Magnetism: Principles and Applications of Enviromagnetics*. San Diego: Academic Press, 2003
- 4 Verosub K L, Roberts A P. Environmental magnetism: Past, present and future. *J Geophys Res*, 1995, 100: 2175–2192
- 5 Hunt C P, Moskowitz B M, Banerjee S K. Magnetic properties of rocks and minerals. In: Ahrens T J, ed. *Rock Physics and Phase Relations: A Handbook of Physical Constants*. Washington D C: American Geophysical Union, 1995. 189–204
- 6 Grousset F E, Labeyrie L, Sinko J A, et al. Patterns of Ice-Rafted Detritus in the Glacial North Atlantic (40°–55°N). *Paleoceanography*, 1993, 8: 175–192
- 7 Verosub K L, Fine P, Singer M J, et al. Pedogenesis and paleoclimate: interpretation of the magnetic susceptibility record of Chinese loess-paleosol sequences. *Geology*, 1993, 21: 1011–1014
- 8 Liu Q S, Deng C L, Yu Y J, et al. Temperature dependence of magnetic susceptibility in an argon environment: implications for pedogenesis of Chinese loess/paleosols. *Geophys J Int*, 2005, 161: 102–112
- 9 Deng C L, Zhu R X, Jackson M J, et al. Variability of the tempera-

- ture-dependent susceptibility of the Holocene eolian deposits in the Chinese loess plateau: A pedogenesis indicator. *Phys Chem Earth A*, 2001, 26: 873–878
- 10 Liu Q S, Torrent J, Maher B A, et al. Quantifying grain size distribution of pedogenic magnetic particles in Chinese loess and significance for pedogenesis. *J Geophys Res*, 2005, 110: B11102, doi: 10.1029/2005JB003726
- 11 Liu Q S, Jackson M J, Yu Y J, et al. Grain size distribution of pedogenic magnetic particles in Chinese loess/paleosols. *Geophys Res Lett*, 2004, 31: L22603, doi: 10.1029/2004GL021090
- 12 Liu Q S, Deng C L. Magnetic susceptibility and its environmental significances (in Chinese). *Chinese J Geophys*, 2009, 52: 1041–1048, doi: 10.3969/j.issn.0001-5733.2009.04.021
- 13 Zhou L P, Oldfield F, Wintle A G, et al. Partly pedogenic origin of magnetic variations in Chinese loess. *Nature*, 1990, 346: 737–739
- 14 Worm H U. On the superparamagnetic-stable single domain transition for magnetite, and frequency dependency of susceptibility. *Geophys J Int*, 1998, 133: 201–206
- 15 Eyre J K. Frequency dependence of magnetic susceptibility for populations of single-domain grains. *Geophys J Int*, 1997, 129: 209–211
- 16 Stephenson A. Single domain grain distributions—A method for the determination of single domain grain distributions. *Phys Earth Planet Inter*, 1971, 4: 353–360
- 17 Liu Q S, Deng C L, Pan Y X. Temperature-dependency and frequency-dependency of magnetic susceptibility of magnetite and maghemite and their significance for environmental magnetism (in Chinese). *Quat Sci*, 2007, 27: 955–962
- 18 Wagner L E, Ding D. Representing aggregate size distributions as modified lognormal distributions. *Trans ASAE*, 1994, 37: 815–821
- 19 Eberl D D, Kile D E, Drits V A. On geological interpretations of crystal size distributions: Constant vs. proportionate growth. *Am Mineral*, 2002, 87: 1235–1241
- 20 Ao H, Deng C L. Review in the identification of magnetic minerals (in Chinese). *Prog Geophys*, 2007, 22: 432–442
- 21 Dunlop D J, Özdemir Ö. *Rock Magnetism: Fundamentals and Frontiers*. Cambridge: Cambridge University Press, 1997
- 22 Muxworthy A R. Effect of grain interactions on the frequency dependence of magnetic susceptibility. *Geophys J Int*, 2001, 144: 441–447
- 23 Sun D H, Bloemendal J, Rea D K, et al. Grain-size distribution function of polymodal sediments in hydraulic and aeolian environments and numerical partitioning of the sedimentary compounds. *Sediment Geol*, 2002, 152: 263–277
- 24 Deng C L, Liu Q S, Pan Y X, et al. Environmental magnetism of Chinese loess-paleosol sequences (in Chinese). *Quat Sci*, 2007, 27: 193–209
- 25 Mørup S, Madsen D E, Frandsen C, et al. Experimental and theoretical studies of nanoparticles of antiferromagnetic materials. *J Phys Condens Matter*, 2007, 19: 213202, doi: 10.1088/0953-8984/19/21/213202